Current-Based Detection of Mechanical Unbalance in an Induction Machine Using Spectral Kurtosis with Reference

Etienne Fournier, Antoine Picot, *Member, IEEE,* Jérémi Régnier, *Member, IEEE,* Mathias TientcheuYamdeu, Jean-Marie Andréjak, and Pascal Maussion, *Member, IEEE,*

***Abstract*—This article explores the design, on-line, of an electrical machine's healthy reference by means of statistical tools. The definition of a healthy reference enables the computation of normalized fault indicators whose value is independent of the system's characteristics. This is a great advantage when diagnosing a broad range of systems with different power, coupling, inertia, load, etc. In this paper, an original method called spectral kurtosis with reference is presented in order to design a system's healthy reference. Its principle is first explained on a synthetic signal. This approach is then evaluated for mechanical unbalance detection in an induction machine using the stator currents instantaneous frequency. The normalized behaviour of the proposed indicator is then confirmed for different operating conditions and its robustness with respect to load variations is demonstrated. Finally, the advantages of using a statistical indicator based on a healthy reference compared to a raw fault signature are discussed.**

***Index Terms*—Spectral Kurtosis, Condition Monitoring, Statistics, Healthy Reference, Normalized Fault Indicator, Mechanical Unbalance, Induction Motor, Instantaneous Frequency, Fault Diagnosis.**

NOMENCLATURE

μ	Mean
σ	Standard Deviation
B_1	Low level of mechanical unbalance
B_2	Medium level of mechanical unbalance
B_3	High level of mechanical unbalance
f_f	Supply frequency
f_r	Rotation frequency
f_s	Sample frequency
$I(t)$	Stator current
$I_\alpha(t)$	Stator current in α-axis
$I_\beta(t)$	Stator current in β-axis
$IA(t)$	Stator current instantaneous amplitude
$IF(t)$	Stator current instantaneous frequency
K	Kurtosis
N_{mov}	Length of the tested set
N_{ref}	Length of the reference set
s	Slip of the induction machine
SK	Spectral kurtosis
SK_R	Spectral kurtosis with reference
$X(f)$	Fourier Transform of variable $X(t)$ at frequency f

E. Fournier is with Leroy Somer, Angoulême, France and the Université de Toulouse, INPT, UPS, LAPLACE (Laboratoire Plasma et Conversion d'Énergie), ENSEEIHT, 2 rue Charles Camichel, BP 7122, F-31071 Toulouse cedex 7, France.

M. Picot, J. Régnier, and P. Maussion are with the Université de Toulouse, INPT, UPS, LAPLACE (Laboratoire Plasma et Conversion d'Énergie), ENSEEIHT, 2 rue Charles Camichel, BP 7122, F-31071 Toulouse cedex 7, France.

M. TientcheuYamdeu and J-M. Andréjak are with Leroy Somer, Angoulême, France.

I. INTRODUCTION

DIAGNOSIS and condition monitoring of electrical machines has become a major topic of concern among industrial and academic research. Unexpected failures in electromechanical systems may indeed lead to important losses of production, safety issues and additional costs. For these reasons, developing efficient and robust diagnosis systems is a priority for electrical machines' manufacturers.

Numerous monitoring methods are based on vibratory signals' analysis and enable an efficient detection of mechanical faults [1]-[4]. However, these methods require accelerometers which are expensive devices. They are only profitable for high power systems where vibration sensors represent a negligible part of the total cost. Therefore, research has focused on diagnosing machine failures through the analysis of current signals due to their availability for control purposes. These methods are mainly based on the Motor Current Signature Analysis (MCSA). A review of MCSA techniques can be found in [5]. These methods generally focus on failures generating fault signatures at specific frequencies. These harmonics are predicted by MCSA and can be tracked with signal processing tools in order to obtain specific fault indicators [6]-[12]. In the case of mechanical unbalance detection, the current spectral signatures at frequencies $f_f \pm f_r$ proved to be efficient fault indicators [13]-[14]. MCSA may also be used on other electrical quantities extracted from stator currents such as active and reactive power [15], current instantaneous frequency [16]-[17] or demodulated current signals [18].

However, recent researches pay little attention to unavoidable constraints faced in diagnosing a manufacturer's broad range of machines. Most works focus on the study of a single machine operating at a particular functioning point but MCSA fault indicators may vary a lot for healthy and faulty conditions depending on the system's characteristics and operating point. For example, Bellini et al. showed in [19] the influence of

the load inertia level on fault signatures related to broken bar detection. It has also been shown in [13] that the load level could significantly affect current signatures linked to mechanical unbalance. Thus, classification systems based on neural networks (NN) or fuzzy logic (FL) have been developed in order to automatically determine a machine's health state while taking into account its characteristics and operating conditions. Relevant applications of NNs based on stator currents are presented in [20]-[23]. Bearing fault detection is also studied by Raj et al. in [24] with a FL-based surveillance system. All these classification methods require faulty and healthy learning sets at different operating points for training. During the functioning time of the system, each new data set is compared to the different learning sets in order to determine the machine's health condition. Fault severity may as well be evaluated if faulty learning sets have been realized for different levels of the considered degradation. Unfortunately, it seems impossible for a machine's manufacturer to obtain such an amount of information, especially faulty learning sets, for every machine model. Moreover, these information may depend on the machine environment such as the load inertia or the coupling for example.

In this context, it seems more profitable to create a machine's healthy reference during its initial working period by statistical means and with a protocol which takes into account the influence of the operating point. After this reference period, each new recording will be tested to find out whether the system has drifted from its referenced behaviour or not. The aim is therefore to detect faulty workings and the estimation of the fault severity is not targeted here since no faulty learning sets are used. The present article explains how new implementations of the spectral kurtosis (SK) make this kind of monitoring possible. SK is a signal processing tool complementing the Power Spectrum Density (PSD) representation. Its rules and properties are explained in [25]. Recent works [26]-[28] have shown that SK may be an efficient tool for monitoring faults generating impulses in vibration or current signals such as bearing or gear faults. Moreover, SK can also be successfully used to detect generalized-roughness bearing fault, as shown in [29]. However, SK is unsuitable for detecting long term changes within a signal in its classic implementation. Indeed, a slowly increasing spectral component is considered as stationary on each local part of the signal by the SK. A different approach is presented in a previous work [30] with new protocols of computation of the SK. These SK calculations no longer use only a single signal's recording but several recordings in order to detect a developing mechanical unbalance in an induction machine (IM) via stator phase currents.

In this context, this article aims to enhance the design of normalized fault indicators independent of a machine's type, power and operating point by using a statistical reference. This healthy reference is provided thanks to the spectral kurtosis with reference (SK_R) presented in [30] and detailed in this paper. Moreover, new experimental tests have been carried out at several load conditions and current instantaneous frequency (IF) is now used to monitor mechanical unbalance development. Applications targeted in this paper are industrial systems such as fans, pumps or compressors driven by induction motors. These latter are fed by open-loop inverters which enable the selection of one or several supply frequencies dedicated to the monitoring phases. In Section II, definition and properties of the classic implementation SK are presented to remind its principle of operation. In section III, the SK_R computation protocol is designed in order to overcome the limitations of the SK. SK_R performance are then tested in Section IV for detection of a developing mechanical unbalance via current IF. These experiments are performed at several load conditions in order to verify the normalized character of SK_R indicators. SK_R robustness when faced to load variations is also tested. Finally, advantages of SK_R for the diagnosis of a broad range of machine are discussed and perspectives are detailed.

II. Mathematical Background and Classical Use of Spectral Kurtosis

A. Kurtosis

Let x be a random variable with mean μ and standard deviation σ. In high order statistics, the *excess kurtosis* of the random variable x is defined in (1) as

$$K(x) = \frac{\kappa_4}{\kappa_2^2} \tag{1}$$

where κ_i is the i^{th} cumulant of x and is defined as

$$\kappa_i = m_i - \sum_{k=0}^{i-1} \binom{k-1}{i-1} \kappa_k m_{i-k} \tag{2}$$

with m_i is the i^{th} moment of x. For clarity reasons, the excess kurtosis will be simply referred as kurtosis from now on.

In statistics, kurtosis is the second shape factor (after the skewness) and reflects the sharpness of a distribution. The sharper the distribution of x, the higher its kurtosis. Reciprocally, the flatter the distribution, the lower its kurtosis. However, kurtosis may also be used to detect outlier elements within a distribution. For instance, let us consider a sample of a random variable x whose probability density function (PDF) is illustrated in Fig. 1 (top). The kurtosis of this sample, where there is no outliers and whose elements are well gathered around the sample's mean, has a low value (examples: 0 for a Gaussian sample, -1,2 for a uniform sample). Now, let us consider the same sample in which were added some extreme (and rare) elements around 10. Its PDF is plotted in Fig. 1 (bottom). This time the sample's kurtosis has a high value caused by the outliers' presence. This property is the basic principle used in SK computation for detecting non-stationary components within a signal.

B. Classic Spectral Kurtosis

Let $x[k] \in \mathbb{R}$ be a digital signal and $X(f)$ its Discrete Fourier Transform. Its spectral component at a specific frequency f_i is a complex random variable, noted $X(f_i)$. Thus, the spectral kurtosis of $x(k)$ is noted $SK_x(f)$ and is defined as the kurtosis of the random variable $X(f_i)$ at each frequency f_i [26]

$$SK_x(f_i) = K(X(f_i)) = \frac{\kappa_4(X(f_i))}{\kappa_2^2(X(f_i))} \tag{3}$$

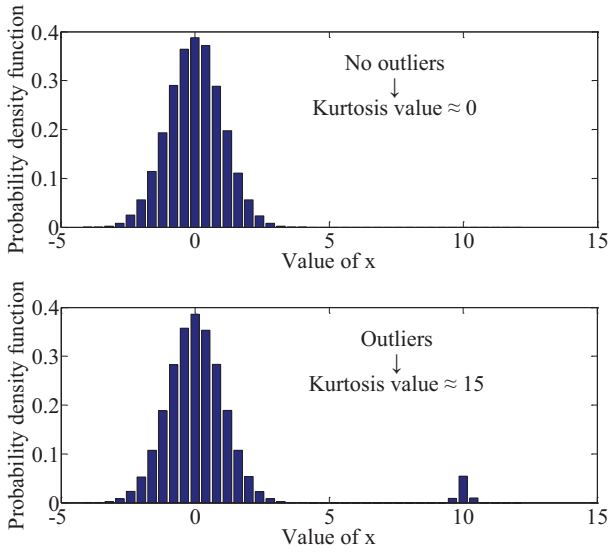

Fig. 1. Probability density function and kurtosis value of a normal distribution without outliers (top) and with some outlier elements around 10 (bottom). The presence of outliers within a distribution is responsible for the increase of its kurtosis value.

Therefore, a minimum number of spectra is required to properly estimate a signal's SK. In practice, this number is reached by using the STFT whose principle is to split the signal x into N segments (with or without overlap) and to compute a FFT on each one. When a spectral component $|X(f)|$ has a stationary behavior, its distribution is similar to the one presented in Fig. 1 (top). Thus, $SK_x(f)$ has a low value. On the contrary, when this spectral component is non-stationary, its distribution is closer to the one presented in Fig. 1 (bottom). More explanations about the principle of operation of SK and its computation protocol are detailed in [30].

This algorithm is therefore suitable to detect fault signatures with a non-stationary behaviour during a recording period, such as bearing faults. However, an innovative SK implementation is presented in the following section in order to design normalized fault indicators for other types of degradation.

III. Definition of a Machine's Healthy Reference via a New Implementation of Spectral Kurtosis

In the case of the monitoring of an electrical machine, phase currents (or other useful measures) are recorded for a certain amount of time $T_{recording}$ at regular intervals, once a day for example. Each recording contains L samples. As shown in section II, SK would be an efficient indicator to detect fault signatures with a non-stationary behaviour over time $T_{recording}$, such as some bearing faults signatures. However, many faults occurring in electro-mechanical systems are more likely to produce signatures with a stationary behaviour. Indeed, a mechanical unbalance slowly increasing in a ventilation system will induce fault signatures growing over large time scale but locally constant on each recording. A shaft misalignment provoked by a maintenance phase would do the same but more suddenly. Therefore, this section focuses on the design of normalized fault indicators with the aim of detecting two successive increases of the level of a simulated mechanical unbalance.

In order to simulate a mechanical unbalance in a rotating system, let us consider a synthetic signal $IF(t)$ representing the current instantaneous frequency. To obtain this variable, $I_\alpha(t)$ and $I_\beta(t)$ are first computed by applying Concordia matrix on phase currents $I_1(t)$, $I_2(t)$ and $I_3(t)$. Instantaneous frequency (IF) and instantaneous amplitude (IA) of stator currents are then defined as

$$IF(t) = \frac{1}{2\pi}\frac{d\phi(t)}{dt} \tag{4}$$

$$IA(t) = |I_c(t)| \tag{5}$$

with $I_c(t) = I_\alpha(t) + iI_\beta(t)$ and $\phi(t) = arg(I_c(t))$. The authors of [14] indeed proved that faults producing load torque oscillation also cause phase modulations (PM) of stator currents. Thus, IF is a relevant quantity for detecting these kinds of faults because it reveals PM harmonics of currents. The impact of a mechanical unbalance on the current IF can reasonably be modelled as

$$IF(t) = f_f + \beta \cdot cos(2\pi f_r t + \phi_r) + n(t) \tag{6}$$

This signal is composed of:

1) a constant component of amplitude $f_f \rightarrow$ the current fundamental frequency;
2) a fault component with an amplitude equal to β at the rotation frequency $f_r \rightarrow$ relative to the unbalance level;
3) a noise component $n(t)$.

In this example, the signal $IF(t)$ is composed of 400 $5s$-recordings and the fault severity β evolves over the recordings as shown in Fig. 2. This profile is representative of two successive increases of the fault component of IF at frequency f_r.

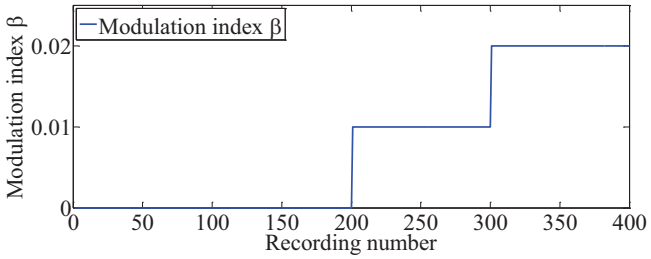

Fig. 2. Evolution of the modulation index (or fault severity) β over the 400 recordings. This profile models two successive increases of the simulated fault severity.

A. Spectral Kurtosis

First, the classical implementation of the SK is tested on the synthetic signal IF. It is computed on each IF recording by using STFT windows of $8000pts$ with 75 % overlap. Specific explanations on the choice of the window length and the overlap are given in [25] and [27]. The SK of the simulated current IF at frequency f_r is presented in Fig. 3. It can be observed that the indicator $SK(f_r)$ decreases from about 0 to -0.8 after the first increase of the modulation

[8] I. X. Bogiatzidis, A. N. Safacas and E. D. Mitronikas, "Detection of Backlash Phenomena Appearing in a Single Cement Kiln Drive Using the Current and the Electromagnetic Torque Signature," *IEEE Trans. on Ind. Electron.*, vol. 60, no. 8, pp. 3441-3453, Aug 2013.

[9] M. Y. Kaikaa and M. Hadjami, "Effects of the Simultaneous Presence of Static Eccentricity and Broken Rotor Bars on the Stator Current of Induction Machine," *IEEE Trans. on Ind. Electron.*, vol. 61, no. 5, pp. 2452-2463, May 2014.

[10] H. Saavedra, J-R. Riba and L. Romeral, "Inter-turn Fault Detection in Five Phases PMSMs. Effects of the Fault Severity," *Proc. of IEEE SDEMPED*, Aug. 2013, pp. 520-526.

[11] T. Ilamparithi and S. Nandi, "Saturation Independent Detection of Dynamic Eccentricity Fault in Salient-pole Synchronous Machines," *Proc. of IEEE SDEMPED*, Aug. 2013, pp. 336-341.

[12] A. J. Fernandez and T. J. Sobczyk, "Motor Current Signature Analysis Apply for External Mechanical Fault and Cage Asymmetry in Induction Motors," *Proc. of IEEE SDEMPED*, Aug. 2013, pp. 136-141.

[13] M. Salah, K. Bacha and A. Chaari, "Stator Current Analysis of a Squirrel Cage Motor Running Under Mechanical Unbalance Condition," *Proc. of IEEE SSD*, Mar. 2013, pp. 1-6.

[14] M. Blodt, M. Chabert, J. Regnier and J. Faucher, "Mechanical Load Fault Detection in Induction Motors by Stator Current Time-Frequency Analysis," *IEEE Trans. on Ind. Appl.*, vol. 42, no. 6, pp. 1454-1463, Nov./Dec. 2006.

[15] M. Drif and A. J. Marquez Cardoso, "Discriminating the Simultaneous Occurence of Three-Phase Induction Motor Rotor Faults and Mechanical Load Oscillations by the Instantaneous Active and Reactive Power Media Signature Analyses," *IEEE Trans. on Ind. Electron.*, vol. 59, no. 3, pp. 1630-1639, Mar. 2012.

[16] B. Trajin, M. Chabert, J. Regnier and J.Faucher, "Hilbert versus Concordia Transform for Three-Phase Machine Stator Current Time-Frequency Monitoring," *MSSP*, vol. 23, no. 8, pp. 2648-2657, Nov. 2009.

[17] S. H. Kia, H. Henao and G. A. Capolino, "Gear Tooth Surface Damage Fault Detection Using Induction Machine Electrical Signature Analysis," *Proc. of IEEE SDEMPED*, Aug. 2013, pp. 358-364.

[18] X. Gong and W. Qiao, "Bearing Fault Diagnosis for Direct-Drive Wind Turbines via Current-Demodulated Signals," *IEEE Trans. on Ind. Electron.*, vol. 60, no. 8, pp. 3419-3428, Aug. 2013.

[19] A. Bellini, C. Concari, G. Franceschini and E. Lorenzani, "Thorough Understanding and Experimental Validation of Current Sideband Components in Induction Machines Rotor Monitoring," *Proc. of IEEE IECON*, Nov. 2006, pp. 4957-4962.

[20] T. Boukra, A. Lebaroud and G. Clerc, "Statistical and Neural-Network Approaches for the Classification of Induction Machine Faults Using the Ambiguity Plane Representation," *IEEE Trans. on Ind. Electron.*, vol. 60, no. 9, pp. 4034-4042, Sep. 2013.

[21] M. Wolkiewicz and C. T. Kowalski, "On-line Neural Network-based Stator Fault Diagnosis System of the Converter-Fed Induction Motor Drive," *Proc. of IEEE IECON*, Nov. 2013, pp. 5561-5566.

[22] S. Toma, L. Capocchi and G. A. Capolino, "Wound-Rotor Induction Generator Inter-Turn Short-Circuits Diagnosis Using a New Digital Neural Network," *IEEE Trans. on Ind. Electron.*, vol. 60, no. 9, pp. 4043-4052, Sep. 2013.

[23] P. J. Broniera, W. S. Gongora, A. Goedtel and W. F. Godoy, "Diagnosis of Stator Winding Inter-turn Short Circuit in Three-Phase Induction Motors by Using Artificial Neural Networks," *Proc. of IEEE SDEMPED*, Aug. 2013, pp. 281-287.

[24] A. S. Raj and N. Murali, "Early Classification of Bearing Faults Using Morphological Operators and Fuzzy Inference," *IEEE Trans. on Ind. Electron.*, vol. 60, no. 2, pp. 567-574, Feb. 2013.

[25] J. Antoni, "The Spectral Kurtosis : a Useful Tool for Characterizing Non-Stationary Signals," *MSSP*, vol. 20, no. 2, pp. 282-307, Feb. 2006.

[26] V. Vrabie, P. Granjon, C. S. Maroni and B. Lepettre, "Application of Spectral Kurtosis to Bearing Fault Detection in Induction Motors," *Proc. of International Conference Surveillance 5*, Oct. 2004.

[27] J. Antoni and R. B. Randall, "The Spectral Kurtosis : Application to the Vibratory Surveillance and diagnostics of rotating machines," *MSSP*, vol. 20, no. 2, pp. 308-331, Feb. 2006.

[28] W. Taiyong and L. Jinhzou, "Fault Diagnosis of Rolling Bearings Based on Wavelet Packet and Spectral Kurtosis," *Proc. of IEEE ICICTA*, Mar. 2011, pp. 665-669.

[29] F. Immovilli, M. Cocconcelli, A. Bellini and R. Rubini, "Detection of Generalized-Roughness Bearing Fault by Spectral-Kurtosis Energy of Vibration or Current Signals," *IEEE Trans. on Ind. Electron.*, vol. 56, no. 11, pp. 4710-4717, Nov. 2009.

[30] E. Fournier, A. Picot, J. Regnier, M. TientcheuYamdeu, J. M. Andrejak and P. Maussion, "On the use of Spectral Kurtosis for Diagnosis of Electrical Machines," *Proc. of IEEE SDEMPED*, Aug. 2013, pp. 77-84.

Etienne Fournier got his MSc in electrical engineering from Supélec Gif-sur-Yvette, France in 2012. He is now a PhD Student at the Laboratory of Plasma and Energy Conversion (LAPLACE) in Toulouse, France. His Scholarship is funded under an industrial agreement with Moteurs Leroy Somer in Angoulême, France. His work focuses on preventive diagnostic of electrical machines under variable-speed control.

Antoine Picot graduated from the Telecom Department of the Institut National Polytechnique (INP) Grenoble, France in 2006. He received the MSc degree in signal, image, speech processing and telecommunications in 2006 and his PhD in automatic control and signal processing in 2009 from the INP Grenoble. He is actually an associate professor at the INP Toulouse. He is also a Researcher with the Laboratory of Plasma and Energy Conversion (LAPLACE), Toulouse. His research interests are in monitoring and diagnosis of complex systems with signal processing and artificial intelligence techniques.

Jérémi Régnier was born in 1975. He received the PhD degree in electrical engineering from the Institut National Polytechnique (INP) Toulouse, France in 2003. Since 2004, he has been an Assistant Professor with the Electrical Engineering and Control Systems Department, INP Toulouse. He is also a Researcher with the Laboratory of Plasma and Energy Conversion (LAPLACE), Toulouse. His research interests include modelling and simulation of faulty electrical systems as well as the development of monitoring techniques using signal-based and model-based methods.

Mathias Tientcheu Yamdeu got his MSc in Electrical Engineering and Automatic control from Institut National Polytechnique (INP) Toulouse, France in 1990. He is currently a senior engineer at Moteurs Leroy Somer in Angoulême, France where he is in charge of the control and diagnostic of variable speed drives and power electronics converters.

Jean-Marie Andréjak got his MSc in Electrical Engineering from ENSEEIHT Toulouse, France in 1978. After having worked in JEUMONT-SCHNEIDER, in electronics E&D department for 10 years, he joined Moteurs Leroy Somer in Angoulême, France, in 1989. He is the Power Electronics E&D manager.

Pascal Maussion got his MSc and PhD in Electrical Engineering in 1985 and 1990 from Institut National Polytechnique (INP) Toulouse, France. He is currently full Professor with the University of Toulouse and with the Laboratory of Plasma and Energy Conversion (LAPLACE), Toulouse. His research activities deal with control and diagnosis of electrical systems (power converters, drives, lighting) and with the design of experiments for optimisation in control and diagnosis. He is currently Head of Control and Diagnosis group in LAPLACE. He teaches control and diagnosis in a school of engineers.

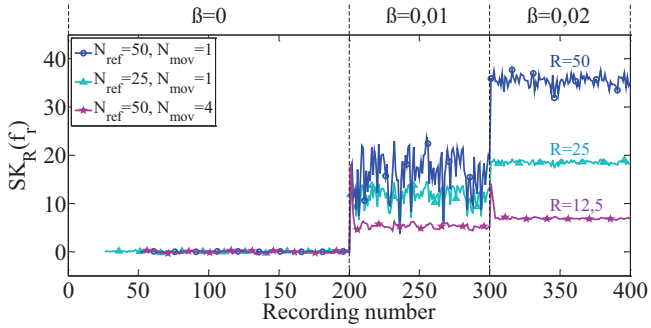

Fig. 5. SK_R applied on the simulated fault harmonic $IF(f_r)$ for $N_{ref} = 50$ and $N_{mov} = 1$ (dark blue line with circles), $N_{ref} = 25$ and $N_{mov} = 1$ (light blue line with triangles) and $N_{ref} = 50$ and $N_{mov} = 4$ (magenta line with stars). The ratio $R = \frac{N_{ref}}{N_{mov}}$ greatly impacts the indicator's behaviour.

excessive because its length also conditions the duration of the reference phase. A good compromise between a trustworthy reference and a short referencing phase is $N_{ref} = 50$. Now let us consider the choice of the parameter N_{mov}. As it is visible in Fig. 5, the reaction of indicator SK_R is strongly related to the ratio $R = \frac{N_{ref}}{N_{mov}}$. Indeed, SK_R reacts stronger for high R values but it is also noisier. In any case, the detection sensitivity is not affected by parameter N_{mov} as long as the ratio R is much higher than 1. $N_{mov} = 1$ is a good choice since it ensures the highest possible value of R for a given value of N_{ref}. In this way, the indicator SK_R tests the membership of the latest value of the considered fault signature to its reference achieved during healthy working. The couple $\{N_{ref} = 50, N_{mov} = 1\}$ is not the unique possibility but the indicator SK_R thus created is robust and easy to interpret. This choice will therefore be retained in the rest of the study.

Finally, an improvement of the SK_R can be easily achieved. It may indeed be useful to subtract the kurtosis value of the reference set to the SK_R value in order to correct the non-Gaussianity of the considered variable. In this way, SK_R has always a quasi-zero value during healthy period, even if the random variable is not Gaussian.

IV. Experimental Results

A. Test Bench Description

An experimental test bench has been set up in order to illustrate the efficiency of SK_R for the detection of a mechanical unbalance occurring in an electro-mechanical system. The experimental bench is composed of:

1) a 5.5 kW *Leroy Somer* IM with two poles pairs, 28 rotor bars and a wye connection;
2) a direct current motor (DCM) used as a generator in order to produce the desired load torque level;
3) an iron disk placed on the shaft between both machines. Several weights may be associated with it in order to create different levels of mechanical unbalance.

An overall view of the test bench is presented in Fig. 6. The IM is fed by an open-loop inverter and all tests presented in this section are realized with a supply frequency $f_f = 40Hz$. A data acquisition system is used to measure the IM phase

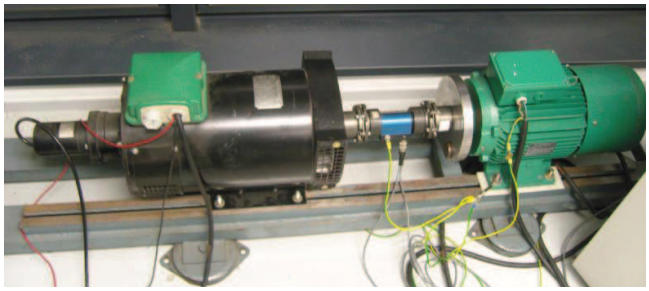

Fig. 6. Experimental test bench composed of a 5.5 kW induction machine (right), a direct current motor to produce the load torque (left) and a iron disk placed on the shaft to create the different levels of mechanical unbalance.

currents with a sample frequency $f_s = 10kHz$ and a digital resolution of 18 bits. Currents recordings are achieved by means of three synchronous channels in order to make the computation of the current IF possible. The unbalance levels B_1, B_2 and B_3 are mechanically generated by means of different weights m_1, m_2 and m_3 placed on the iron disk as illustrated in Fig. 7. A weight m attached at a distance R from

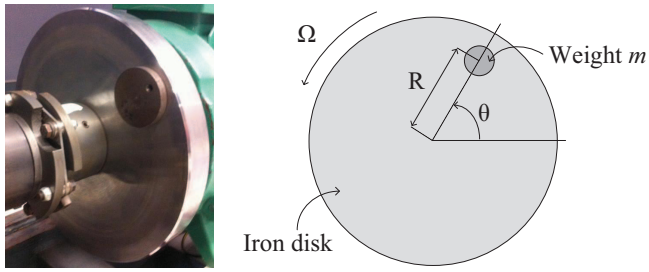

Fig. 7. Photography (left) and schematic representation (right) of the iron disk used to generate the three levels of mechanical unbalance B_1, B_2 and B_3. The different weights m_1, m_2 and m_3 are attached on the iron disk at a distance R from the rotation axis in order to generate the desired level of mechanical unbalance.

the system's rotation axis generates load torque oscillations $\Gamma_{osc}(t)$ at the frequency rotation f_r which are defined by

$$\Gamma_{osc}(t) = m \cdot R \cdot g \cdot cos(2\pi f_r t) \quad (7)$$

with g the gravitational acceleration. For example, this kind of degradation usually happens in industrial fans due to blade clogging by grease and dust accumulation or the break of a fan blade. Once detected, the mechanical unbalance may easily be fixed in order to prevent a premature wear of the mechanical components, especially bearings.

B. Tests at no load condition

250 5s-recordings of the IM currents have been measured on the machine. They are composed of:

1) 100 recordings with no mechanical unbalance and corresponding to the healthy state of the machine;
2) 50 recordings with the low level of mechanical unbalance B_1 created by a small weight $m_1 = 77.5g$ fixed to the iron disk at a distance $R = 7.5cm$ from the rotation axis. This level of mechanical unbalance produces load

torque oscillations at f_r with a theoretical amplitude of 0.15% of the IM rated torque;

3) 50 recordings with the medium level of mechanical unbalance B_2 created by a small weight $m_2 = 133g$ fixed to the iron disk at a distance $R = 7.5cm$ from the rotation axis. This level of mechanical unbalance produces load torque oscillations at f_r with a theoretical amplitude of 0.27% of the IM rated torque;
4) 50 recordings with the high level of mechanical unbalance B_3 created by a small weight $m_3 = 274g$ fixed to the iron disk at a distance $R = 7.5cm$ from the rotation axis. This level of mechanical unbalance produces load torque oscillations at f_r with a theoretical amplitude of 0.55% of the IM rated torque.

The spectral component of the current IF at frequency f is noted $\hat{IF}(f)$. It is shown in [14] that a mechanical unbalance produces a phase modulation (PM) of the current fundamental (of frequency f_f) at the rotation frequency f_r. So, mechanical unbalance signature appears in the current IF spectrum at frequency f_r. In order to tolerate small variations of the system operating point while monitoring spectral components, we redefine the variable $IF(f)$ as

$$IF(f) = max\{\hat{IF}(f - \Delta f : f + \Delta f)\} \quad (8)$$

with Δf chosen to be $0.2Hz$. In this case, $IF(f)$ corresponds to the maximal value of the current spectrum in the frequency range $[f - \Delta f, f + \Delta f]$. The spectral component $IF(f_r)$ have been computed for the 250 recordings and results are plotted in Fig. 8. It is first visible in Fig. 8 that IF is indeed a proper

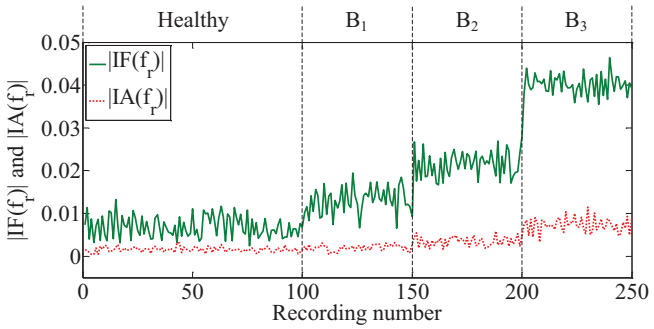

Fig. 8. Illustration of $|IF(f_r)|$ (green solid line) and $|IA(f_r)|$ (red dotted line) evolutions for the different health states of the induction machine (healthy, B_1, B_2 and B_3).

variable for the detection of load torque oscillations due to a mechanical unbalance. Although the harmonic $IF(f_r)$ is noisy, its value remains stable during the healthy working period. Then, its evolution well reflects the different stages of mechanical unbalance. Even the lowest unbalance level visibly affects the mean level of $IF(f_r)$ while it produces extremely weak load oscillations. The harmonic $IA(f_r)$ has also been illustrated in Fig. 8. It can be noticed that IA also reflects the increase of the mechanical unbalance level (especially the two highest levels), but to a much lower extent than IF. Indeed, IA is more sensitive to degradation generating amplitude modulation (AM) of phase currents, such as eccentricity faults. Thus, a joint study of IF and IA may enable the detection and differentiation of many mechanical faults occurring in a system.

However, although it may seem easy to choose a fault threshold for the fault indicator $IF(f_r)$, the healthy level of this harmonic depends on many factors. Electrical machines with different rated power, poles number, inertia, etc... may have different healthy levels of fault signatures. In order to illustrate this issue, let us monitor the harmonic $IF(f_r)$ during two experiments, both in healthy conditions and at the same load level but with two different total inertia. The difference of inertia in the two experiments is only due to the addition of the iron disk on the shaft. Of course, no unbalance weights were fastened on the iron disk during this test. Results of both indicators are shown in Fig. 9. It is well perceptible

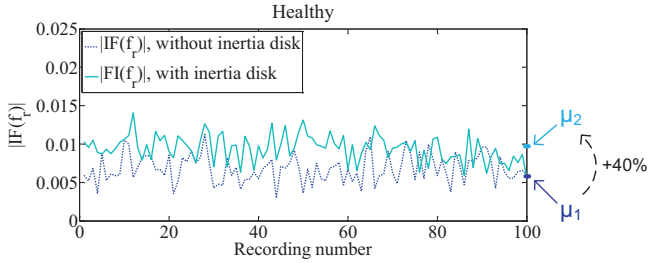

Fig. 9. Fault signature $|IF(f_r)|$ during healthy conditions with different configuration of the monitored system : with the inertia disk (light blue solid line) and without the inertia disk (dark blue dotted line).

in Fig. 9 that both healthy indicators have different mean values $\mu_1 = 0.0068$ and $\mu_2 = 0.0094 \approx 1.4\mu_1$, while the same machine was monitored at the same load level. When considering diagnosis of a broad range of machines and applications, choosing an *a priori* robust fault threshold is therefore tricky. It seems unavoidable to study the behavior of fault signatures during the initial working period of the system, when it can be considered as healthy. In this way, the system's reference created is thus specific to each monitored system, which is a key point of the proposed approach.

It has been shown in section III that SK_R can be used both to create a system's reference and to compare each new recording to it. This second step enables the user to evaluate if the system has drifted from its healthy reference or not. In order to test SK_R efficiency for the detection of a mechanical unbalance, this algorithm has been computed on the fault signature $IF(f_r)$. This computation has been achieved according to the protocol presented in Fig. 4 with $N_{ref} = 50$ and $N_{mov} = 1$. Results are shown in Fig. 10 (green solid line). First, it is visible in Fig. 10 that SK_R is an efficient indicator for detecting the different levels of mechanical unbalance. This statistical treatment holds the information contained in the fault signature $IF(f_r)$. However it normalizes the healthy values around 0 which makes the detection of abnormal behaviours easier. After the reference period, the $SK_R(f_r)$ value remains close to 0 during the healthy operation period. Its value then increases with the severity of the mechanical unbalance. The application of the SK_R on the fault signature $IF(f_r)$ thus enables the creation of a normalized fault indicator. Indeed, SK_R-based indicators

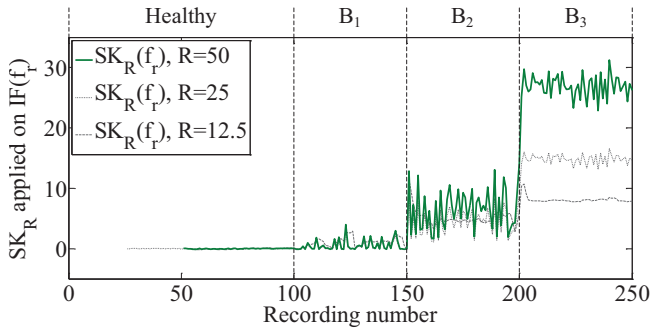

Fig. 10. SK_R applied on current IF at fault frequency f_r in the healthy state and for the different unbalance levels B_1, B_2 and B_3. Different values of the ratio $R = \frac{N_{ref}}{N_{mov}}$ are used and simulation results are confirmed.

will always have a value about equal to zero during healthy condition whereas classical energy indicators may have many different levels, depending on the system characteristics (type of motor, operating point, etc.). This point is major when considering the diagnosis of a wide range of electro-mechanical systems. Finally, the influence of the ratio $R = \frac{N_{ref}}{N_{mov}}$ on the SK_R is experimentally verified. SK_R sensitivity is indeed directly related to the R level. The choice $N_{ref} = 50$ and $N_{mov} = 1$ guarantees a good detection sensitivity and an easy interpretation. It will be conserved in the rest of the study.

C. Tests at different load conditions

The same experiments have been carried out for multiple load conditions in order to confirm the previous results. As mentioned in section IV-B, the application of SK_R on fault signatures enables the creation of normalized fault indicators. But also, a single fault threshold may be associated to these normalized indicators, whatever the system or the fault considered. Indeed, let $SK_R(f_r)$ be the SK_R applied on current IF at frequency f_r. The fault threshold $t_{1\%}$ is defined by

$$\mathbb{P}(SK_R(f_r) > t_{1\%}) = 1\% \tag{9}$$

Therefore, the normalized fault indicator $SK_R(f_r)$ exceeds $t_{1\%}$ only 1% of the time during healthy working conditions. If the exceeding rate of $SK_R(f_r)$ above $t_{1\%}$ is much more higher than 1%, the system has then drifted from its healthy reference. A maintenance phase is thus necessary. For $N_{ref} = 50$ and $N_{mov} = 1$, the fault threshold $t_{1\%}$ is about equal to 0.2.

For every experiment at the different load levels, SK_R has been computed on the fault component $IF(f_r)$. The percentage by which SK_R exceeds the fault threshold $t_{1\%}$ is then calculated for each health state (healthy, lowest unbalance (B_1), middle unbalance (B_2) and highest unbalance (B_3)). The results of this test campaign are presented in Table I. First, it can noticed that, as expected, the exceeding rate of SK_R is always about equal to 1 % during healthy conditions. It is a key point of this reference-based monitoring system because no false alarms are generated, for all load conditions. Then, it can also be observed that the indicator sensitivity seems to decrease with the load level. Indeed, the lowest unbalance level B_1, which is extremely low, is only clearly detectable at no load condition. Two reasons may explain the loss of $SK_R(f_r)$ sensitivity with the load level. First, energy indicators are more noisy for high load levels. Then, their faulty levels also decrease with the increase of the load level. However, both unbalance levels B_2 and B_3 seems well detectable for every load conditions (except the middle unbalance level at 70% load).

TABLE I
PERCENTAGE BY WHICH THE INDICATOR SK_R APPLIED ON $IF(f_r)$ EXCEEDS THE FAULT THRESHOLD $t_{1\%}$ FOR EACH HEALTH STATE AND LOAD LEVEL.

		Load level (% of rated load)					
	Health state	0%	25%	35%	45%	60%	70%
SK_R applied on $IF(f_r)$	Healthy	0	0	1	0	1	0
	B_1	44	7	0	0	1	2
	B_2	100	100	68	42	72	9
	B_3	100	100	100	100	100	100

D. Toward an automatic referencing and monitoring protocol in the torque-speed plane

The previous tests proved the normalization and sensitivity properties of the SK_R at different load conditions. However, a reference was necessary per operating point in order to ensure the proper functioning of the indicator. It is impossible, in practice, to associate a reference per every possible working point in the torque-speed plane because it would require a infinite number of references.

The aim here is therefore to associate a reference to a relatively large area in the torque-speed plane, and not to a singularity. To achieve this, areas must be designed such that the considered fault signature has a stable behaviour on each of them. Experimental results showed that the healthy level of the fault signature $IF(f_r)$ varies moderately with the load level. At a specific supply frequency f_f, the load axis may therefore be split into M relatively large zones and a reference is created per load area.

Experimental results also showed that the healthy level of the considered fault signature could have large variations along the speed axis. To ensure a good robustness and sensitivity of the SK_R indicator, it should be split into a great number of speed zones. However, most industrial systems such as fans, pumps, or compressors, which are targeted in this study, are fed by open-loop inverters. This way, the supply frequency f_f may be changed during the monitoring phases in order to always realize the diagnosis at one or a few supply frequencies.

The tests presented in section IV-C can be reorganized by selecting an adequate division of the load axis and a specific supply frequency chosen to perform the diagnosis phases. The monitoring parameters have been selected as follows:

1) the supply frequency selected to achieve the monitoring phases is equal to $f_f = 40Hz$;
2) the load axis is split into $M = 4$ areas wide by 25% of the rated load.

In this way, a unique reference of the fault signature $IF(f_r)$ is designed for each quarter of the load axis. The reference of the first quarter is built by using N_{ref} recordings acquired at both 0% and 25% of the rated load. In the same way, the reference of the second quarter is designed with N_{ref} values of the fault signature $IF(f_r)$ extracted from recordings at both 35% and 45% of the rated load. Similarly, the reference of the third quarter of the load axis is achieved by using the recordings obtained at 60% and 70% of the rated load. At each new recording, the SK_R applied on the fault signature $IF(f_r)$ is computed by using the reference corresponding to the load level of the system. The percentage by which SK_R exceeds the fault threshold $t_{1\%}$ is then calculated for each health state (healthy, lowest unbalance (B_1), middle unbalance (B_2) and highest unbalance (B_3)) and for the different load areas. Results are presented in Table II. It can be noticed that the false

TABLE II
PERCENTAGE BY WHICH THE INDICATOR SK_R APPLIED ON $IF(f_r)$ EXCEEDS THE FAULT THRESHOLD $t_{1\%}$ FOR EACH HEALTH STATE AND LOAD AREA.

		Load area (% of rated load)		
	Health state	[0%→25%]	[25%→50%]	[50%→75%]
SK_R applied on $IF(f_r)$	Healthy	0	1	1
	B_1	20	1	3
	B_2	99	47	41
	B_3	100	100	100

alarm rate is not affected at all by using a single reference per load area. The robustness of the proposed approach is therefore maintained. Moreover, the SK_R sensitivity is hardly affected by the use of a reference covering a wide zone of the load axis. Indeed, the exceeding rate in a load area is often close to the mean of the exceeding rates of each functioning point included to this area. For example, the exceeding rate under the lowest unbalance level B_1 in the first load quarter is equal to 20. The exceeding rate at 0% of the rated load and the one at 25%, presented in Table I are respectively equal to 44% and 7% giving a mean exceeding rate equal to 25.5%. Both values are close and the little loss of sensitivity observed is due to the slight non-homogeneity of the variable $IF(f_r)$ over the considered load area. Finally, this referencing process could be repeated for different supply frequencies in order to minimize the impact on the application.

To conclude this experimental section, SK_R seems to be an efficient monitoring protocol for the diagnosis of a broad range of induction machines operating with different characteristics (type of load, inertia, coupling, etc.). It should be recalled that the tested unbalance levels remains rather low, from $B_1 = 0.15\%$ to $B_3 = 0.55\%$ of the IM nominal torque. The test campaign presented in Table I shows that a single fault threshold with a statistical meaning is sufficient to ensure a robust detection of these different levels of mechanical unbalance without false alarms. The creation of several references (one for each load condition) enables a good detection of low levels of mechanical unbalances. Because references are created online, SK_R indicator is therefore independent of the type of machine, of load characteristics and others parameters which can affect classical MCSA indicators as the ones presented in Fig. 8. Moreover, tests realized in section IV-D showed that this method may easily be adapted to ensure a robust diagnosis in the torque-speed plane.

V. CONCLUSION

In this paper, an efficient diagnosis protocol based on the computation of a system's healthy reference has been presented. Normalized indicators well adapted for the condition monitoring of a broad range of machines were designed thanks to this statistical reference. In section II, the kurtosis has been defined and its ability to detect outliers within a reference distribution has been demonstrated. In section III, an innovative indicator, the SK_R, based on the kurtosis has been designed by including a reference set. SK_R ability to generate a system's healthy reference and to detect any drift from it has been tested on synthetic signals. Finally, an experimental test bench has been set-up in order to verify SK_R efficiency, when applied on current IF, for the detection of low levels of mechanical unbalance. Tests performed at several load conditions have proven the SK_R detection capacity with a single fault threshold for all load conditions. The creation of the system's healthy reference thus enabled a robust detection of weak mechanical unbalances without any false alarms for different operating conditions. Moreover, its robustness to load variations has been demonstrated.

Future work will focus on the definition a generic monitoring protocol in the torque-speed plane which specifies the references' area of validity and optimizes the indicator's sensitivity while conserving its robustness and minimizing the impact of the monitoring protocol on the application. Moreover, the proposed approach showed good performance for mechanical unbalance detection in an IM and it will be interesting to confirm these results for other kinds of faults (eccentricity, bearing faults, etc.) and for different systems.

REFERENCES

[1] M. D. Prieto, G. Cirrincione, A. G. Espinosa, J. A. Ortega and H. Henao, "Bearing Fault Detection by a Novel Condition-Monitoring Scheme Based on Statistical-Time Features and Neural Networks," *IEEE Trans. on Ind. Electron.*, vol. 30, no. 8, pp. 3398-3407, Aug. 2013.

[2] A. Soualhi, G. Clerc, H. Razik and F. Rivas, "Long-term Prediction of Bearing Condition by the Neo-Fuzzy Neuron," *Proc. of IEEE SDEMPED*, Aug. 2013, pp. 586-591.

[3] J. Harmouche, C. Delpha and D. Diallo, "A Global Approach for the Classification of Bearing Faults Conditions Using Spectral Features," *Proc. of IEEE IECON*, Nov. 2013, pp. 7352-7357.

[4] F. Immovilli, C. Bianchini, M. Cocconcelli , A. Bellini and R. Rubini, "Bearing Fault Model for Induction Motor With Externally Induced Vibration," *IEEE Trans. on Ind. Electron.*, vol. 60, no. 8, pp. 3408-3418, Aug. 2013.

[5] A. Bellini, F. Filippetti, C. Tassoni and G-A. Capolino, "Advances in Diagnostic Techniques for Induction Machines," *IEEE Trans. on Ind. Electron.*, vol. 55, no. 12, pp. 4109-4126, Dec. 2008.

[6] B. M. Ebrahimi, M. J. Roshtkhari, J. Faiz and S. V. Khatami, "Advanced Eccentricity Fault Recognition in Permanent Magnet Synchronous Motors Using Stator Current Signature Analysis," *IEEE Trans. on Ind. Electron.*, vol. 61, no. 4, pp. 2041-2052, Apr. 2014.

[7] G. M. Joksimovic, J. Riger, T. M. Wolbank, N. Peric and M. Vasak, "Stator-Current Spectrum Signature of Healthy Cage Rotor Induction Machines," *IEEE Trans. on Ind. Electron.*, vol. 60, no. 9, pp. 4025-4033, Sep. 2013.

[8] I. X. Bogiatzidis, A. N. Safacas and E. D. Mitronikas, "Detection of Backlash Phenomena Appearing in a Single Cement Kiln Drive Using the Current and the Electromagnetic Torque Signature," *IEEE Trans. on Ind. Electron.*, vol. 60, no. 8, pp. 3441-3453, Aug 2013.

[9] M. Y. Kaikaa and M. Hadjami, "Effects of the Simultaneous Presence of Static Eccentricity and Broken Rotor Bars on the Stator Current of Induction Machine," *IEEE Trans. on Ind. Electron.*, vol. 61, no. 5, pp. 2452-2463, May 2014.

[10] H. Saavedra, J-R. Riba and L. Romeral, "Inter-turn Fault Detection in Five Phases PMSMs. Effects of the Fault Severity," *Proc. of IEEE SDEMPED*, Aug. 2013, pp. 520-526.

[11] T. Ilamparithi and S. Nandi, "Saturation Independent Detection of Dynamic Eccentricity Fault in Salient-pole Synchronous Machines," *Proc. of IEEE SDEMPED*, Aug. 2013, pp. 336-341.

[12] A. J. Fernandez and T. J. Sobczyk, "Motor Current Signature Analysis Apply for External Mechanical Fault and Cage Asymmetry in Induction Motors," *Proc. of IEEE SDEMPED*, Aug. 2013, pp. 136-141.

[13] M. Salah, K. Bacha and A. Chaari, "Stator Current Analysis of a Squirrel Cage Motor Running Under Mechanical Unbalance Condition," *Proc. of IEEE SSD*, Mar. 2013, pp. 1-6.

[14] M. Blodt, M. Chabert, J. Regnier and J. Faucher, "Mechanical Load Fault Detection in Induction Motors by Stator Current Time-Frequency Analysis," *IEEE Trans. on Ind. Appl.*, vol. 42, no. 6, pp. 1454-1463, Nov./Dec. 2006.

[15] M. Drif and A. J. Marquez Cardoso, "Discriminating the Simultaneous Occurence of Three-Phase Induction Motor Rotor Faults and Mechanical Load Oscillations by the Instantaneous Active and Reactive Power Media Signature Analyses," *IEEE Trans. on Ind. Electron.*, vol. 59, no. 3, pp. 1630-1639, Mar. 2012.

[16] B. Trajin, M. Chabert, J. Regnier and J.Faucher, "Hilbert versus Concordia Transform for Three-Phase Machine Stator Current Time-Frequency Monitoring," *MSSP*, vol. 23, no. 8, pp. 2648-2657, Nov. 2009.

[17] S. H. Kia, H. Henao and G. A. Capolino, "Gear Tooth Surface Damage Fault Detection Using Induction Machine Electrical Signature Analysis," *Proc. of IEEE SDEMPED*, Aug. 2013, pp. 358-364.

[18] X. Gong and W. Qiao, "Bearing Fault Diagnosis for Direct-Drive Wind Turbines via Current-Demodulated Signals," *IEEE Trans. on Ind. Electron.*, vol. 60, no. 8, pp. 3419-3428, Aug. 2013.

[19] A. Bellini, C. Concari, G. Franceschini and E. Lorenzani, "Thorough Understanding and Experimental Validation of Current Sideband Components in Induction Machines Rotor Monitoring," *Proc. of IEEE IECON*, Nov. 2006, pp. 4957-4962.

[20] T. Boukra, A. Lebaroud and G. Clerc, "Statistical and Neural-Network Approaches for the Classification of Induction Machine Faults Using the Ambiguity Plane Representation," *IEEE Trans. on Ind. Electron.*, vol. 60, no. 9, pp. 4034-4042, Sep. 2013.

[21] M. Wolkiewicz and C. T. Kowalski, "On-line Neural Network-based Stator Fault Diagnosis System of the Converter-Fed Induction Motor Drive," *Proc. of IEEE IECON*, Nov. 2013, pp. 5561-5566.

[22] S. Toma, L. Capocchi and G. A. Capolino, "Wound-Rotor Induction Generator Inter-Turn Short-Circuits Diagnosis Using a New Digital Neural Network," *IEEE Trans. on Ind. Electron.*, vol. 60, no. 9, pp. 4043-4052, Sep. 2013.

[23] P. J. Broniera, W. S. Gongora, A. Goedtel and W. F. Godoy, "Diagnosis of Stator Winding Inter-turn Short Circuit in Three-Phase Induction Motors by Using Artificial Neural Networks," *Proc. of IEEE SDEMPED*, Aug. 2013, pp. 281-287.

[24] A. S. Raj and N. Murali, "Early Classification of Bearing Faults Using Morphological Operators and Fuzzy Inference," *IEEE Trans. on Ind. Electron.*, vol. 60, no. 2, pp. 567-574, Feb. 2013.

[25] J. Antoni, "The Spectral Kurtosis : a Useful Tool for Characterizing Non-Stationary Signals," *MSSP*, vol. 20, no. 2, pp. 282-307, Feb. 2006.

[26] V. Vrabie, P. Granjon, C. S. Maroni and B. Lepettre, "Application of Spectral Kurtosis to Bearing Fault Detection in Induction Motors," *Proc. of International Conference Surveillance 5*, Oct. 2004.

[27] J. Antoni and R. B. Randall, "The Spectral Kurtosis : Application to the Vibratory Surveillance and diagnostics of rotating machines," *MSSP*, vol. 20, no. 2, pp. 308-331, Feb. 2006.

[28] W. Taiyong and L. Jinhzou, "Fault Diagnosis of Rolling Bearings Based on Wavelet Packet and Spectral Kurtosis," *Proc. of IEEE ICICTA*, Mar. 2011, pp. 665-669.

[29] F. Immovilli, M. Cocconcelli, A. Bellini and R. Rubini, "Detection of Generalized-Roughness Bearing Fault by Spectral-Kurtosis Energy of Vibration or Current Signals," *IEEE Trans. on Ind. Electron.*, vol. 56, no. 11, pp. 4710-4717, Nov. 2009.

[30] E. Fournier, A. Picot, J. Regnier, M. TientcheuYamdeu, J. M. Andrejak and P. Maussion, "On the use of Spectral Kurtosis for Diagnosis of Electrical Machines," *Proc. of IEEE SDEMPED*, Aug. 2013, pp. 77-84.

Etienne Fournier got his MSc in electrical engineering from Supélec Gif-sur-Yvette, France in 2012. He is now a PhD Student at the Laboratory of Plasma and Energy Conversion (LAPLACE) in Toulouse, France. His Scholarship is funded under an industrial agreement with Moteurs Leroy Somer in Angoulême, France. His work focuses on preventive diagnostic of electrical machines under variable-speed control.

Antoine Picot graduated from the Telecom Department of the Institut National Polytechnique (INP) Grenoble, France in 2006. He received the MSc degree in signal, image, speech processing and telecommunications in 2006 and his PhD in automatic control and signal processing in 2009 from the INP Grenoble. He is actually an associate professor at the INP Toulouse. He is also a Researcher with the Laboratory of Plasma and Energy Conversion (LAPLACE), Toulouse. His research interests are in monitoring and diagnosis of complex systems with signal processing and artificial intelligence techniques.

Jérémi Régnier was born in 1975. He received the PhD degree in electrical engineering from the Institut National Polytechnique (INP) Toulouse, France in 2003. Since 2004, he has been an Assistant Professor with the Electrical Engineering and Control Systems Department, INP Toulouse. He is also a Researcher with the Laboratory of Plasma and Energy Conversion (LAPLACE), Toulouse. His research interests include modelling and simulation of faulty electrical systems as well as the development of monitoring techniques using signal-based and model-based methods.

Mathias Tientcheu Yamdeu got his MSc in Electrical Engineering and Automatic control from Institut National Polytechnique (INP) Toulouse, France in 1990. He is currently a senior engineer at Moteurs Leroy Somer in Angoulême, France where he is in charge of the control and diagnostic of variable speed drives and power electronics converters.

Jean-Marie Andréjak got his MSc in Electrical Engineering from ENSEEIHT Toulouse, France in 1978. After having worked in JEUMONT-SCHNEIDER, in electronics E&D department for 10 years, he joined Moteurs Leroy Somer in Angoulême, France, in 1989. He is the Power Electronics E&D manager.

Pascal Maussion got his MSc and PhD in Electrical Engineering in 1985 and 1990 from Institut National Polytechnique (INP) Toulouse, France. He is currently full Professor with the University of Toulouse and with the Laboratory of Plasma and Energy Conversion (LAPLACE), Toulouse. His research activities deal with control and diagnosis of electrical systems (power converters, drives, lighting) and with the design of experiments for optimisation in control and diagnosis. He is currently Head of Control and Diagnosis group in LAPLACE. He teaches control and diagnosis in a school of engineers.